E_LIBANS 2018 Activity

R. Bedogni (Resp.)

J.M. Gomez-Ros (Ass.), A. Pietropaolo (Ass.), W. Plastino (Ass.), A. Filabozzi (Ass.),
K. Alikaniotis (Ass.).

In collaboration with LNF *Servizio Progettazione e Costruzioni Meccaniche*
INFN- LNF

In collaboration with:
Trieste, Torino and Milano INFN sections
ENEA C.R. Frascati (Frascati Neutron Generator)

1 Introduction

The e_LiBANS project started in 2016 to develop homogenous and intense neutron fields, with well-defined and characterize neutron spectra, for interdisciplinary applications. E_LIBANS primary neutron source is a reconditioned, medical-type, ELEKTA SL18 MV electron LINAC installed and re-commissioned in an existing bunker at the Physics Department of University of Torino (Figure 1) [1].
Neutrons are produced through (gamma, n) and (e, n) photon nuclear reactions in a tungsten target plus an added lead target. This neutron production part is followed by an attenuator, which material composition and size were optimized according to the purpose of producing thermal neutrons (E < 0.4 eV), or epithermal neutrons (eV < E < 100 keV).

For the first phase of the project (2016 and 2017), the LINAC was dedicated to the production and characterization of thermal neutron fields. Thus, a photoconverter made of graphite and heavy water was employed. The irradiation volume was a closed cavity, tuneable in size, with maximum dimension 30 cm x 30 cm x 20 cm. Specific thermal neutron diagnostics, all sensitized to thermal neutron through a ^{6}LiF deposition, were designed and commissioned at LNF. These are Silicon-based TNRD (thermal neutron rate detector) and Silicon carbide detectors. To match the characteristics of the field (fluence rate in the 2E+6 cm^{-2} s^{-1}, large accompanying photon background, and large electromagnetic noise), these diagnostics were operated in current mode. This relies on a dedicated ultralow current analogue board that drives the radiation-induced current (tens of fA or higher) to a resistor, making it measurable as a voltage drop [2].

The 2018 activity was focused on:

- spatial mapping of the LINAC-based thermal neutron field
- using the LINAC to produce epithermal neutron fields, according to a previously optimized computational model, and to develop the associated epithermal neutron diagnostics.

The scheme of the epithermal photoconverter is reported in Figure 2. It consists of a graphite, Teflon and aluminium block with size 0.8 m x 0.8 m x 0.8 m. The irradiation volume is a closed cavity, tuneable in size, with maximum dimension 30 cm x 30 cm x 20 cm. The expected neutron spectrum is reported in Figure 3. As shown by Figure 3, the spectrum is nearly pure epithermal, as more than 90% of the fluence is between 1 eV and 100 keV. The total epithermal fluence rate is expected to be 4.8E+5 cm^{-2} s^{-1}.

The LNF were in charge for:

- development of a radionuclide source-based epithermal neutron field for testing the diagnostics

(epithermal neutron metrology);

- development of epithermal neutron detectors suited for monitoring the E_LIBANS epithermal field;
- designing and assembling a 4x4 2D array of Silicon Carbide detectors for the spatial mapping of the E_LIBANS thermal field.

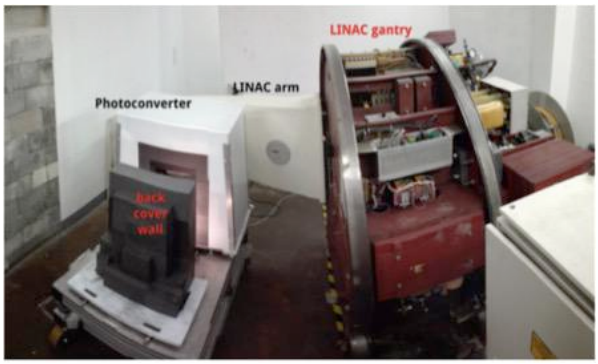

Figure 1. E_LIBANS experimental hall in Torino.

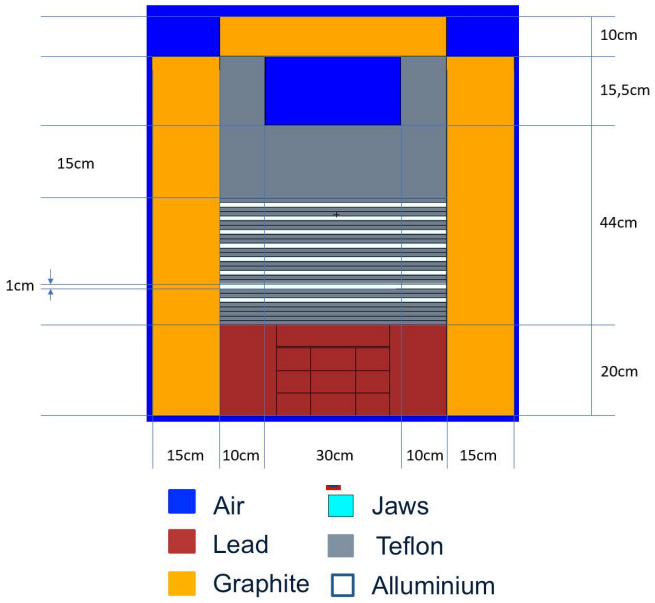

Figure 2. E_LIBANS epithermal photoconverter. The irradiation volume is the blue (air) cavity on top.

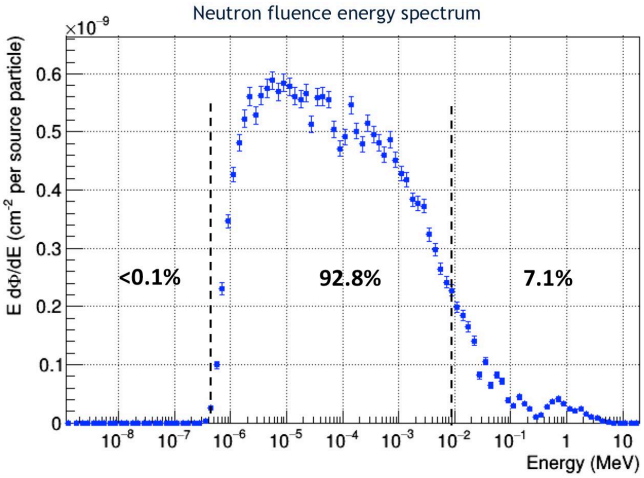

Figure 3. Expected neutron spectrum in the E_LIBANS epithermal cavity.

2 The epithermal neutron field EPINES in Frascati (ENEA / INFN)

2.1 Previous Activity

The first version of E_LIBANS epithermal reference field, called EPINES (EPIthermal neutron source), was developed in 2017 within INFN-LNF / ENEA Frascati collaboration, in the experimental hall of the Frascati Neutron Generator (ENEA Frascati). Characteristics of EPINES field were:

- easy access
- low cost (adapting an existing facility)
- based on radionuclide neutron sources, to guarantee beam stability
- Simple geometry and set-up, to facilitate accurate Monte Carlo modelling and experimental validation

EPINES was developed in collaboration with ENEA Frascati (providing logistics, location, and an existing Am-Boron source) and INFN-Energy (providing the reflecting materials, shared with the NEPED project). EPINES was built by modifying the existing HOTNES thermal neutron facility [3, 4, 5] previously developed by INFN (NEURAPID and E_LIBANS projects) in collaboration with ENEA Frascati. HOTNES, as shown in Figure 4, is a cylindrical cavity with polyethylene walls. An ^{241}Am-B source, located on the facility bottom, feeds the facility. Due to the polyethylene shadow-bar, fast neutrons cannot directly reach the irradiation volume. Only wall-scattered neutrons can reach the irradiation volume instead, and their spectrum is highly thermalized.

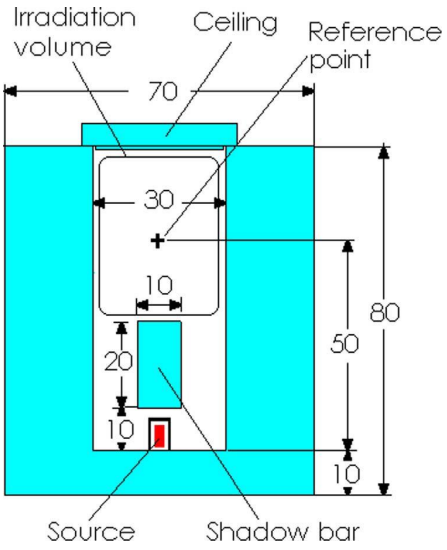

Figure 4. HOTNES internal structure.

Epithermal fields are traditionally achieved by modifying fast neutron fields with "epithermal filters". The epithermal filter should

- eliminate thermal neutrons
- slow down fast neutrons into epithermal neutron
- have a low absorption cross section, thus Hydrogen should be avoided.
- produce few gammas.

Media containing C, F, and Al have been used in epithermal filters [4].
Based on extensive Monte Carlo simulations with MCNPX, two modification schemes were applied to HOTNES in order to obtain a nearly epithermal field in the irradiation cavity. These were characterized by different energy distribution and neutron fluence rate. inside HOTNES cavity. **These configurations were called EPINES / EPI22-c and EPINES / EPI41-c (where "-c" means closed cavity)** and were achieved during the 2017 activity.

EPINES, configuration EPI22-c

HOTNES internal cavity was lined with borated rubber and the length of the shadow-bar was increased from 20 cm to 30 cm, see Fig. 3. The irradiation volume is the upper part of the internal cavity.

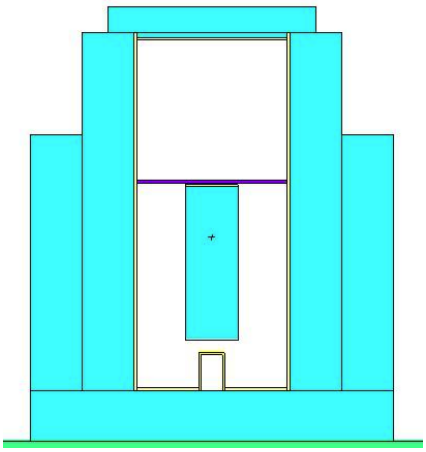

Figure 5. From HOTNES to EPINES, configuration EPI22-c. HOTNES internal cavity was lined with borated rubber (red) and the length of the shadow-bar was increased from 20 cm to 30 cm. Blue indicates polyethylene.

EPINES, configuration EPI41-c

HOTNES internal cavity was lined with borated rubber and the polyethylene shadow-bar was replaced by a multilayer of Teflon (CF2n, 5 cm thick layers) and Aluminium (2.5 cm thick layers). The irradiation volume is the upper part of the internal cavity, See Fig. 6.

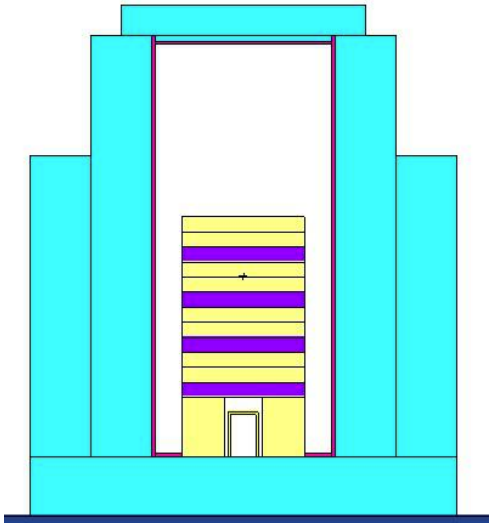

Figure 6. From HOTNES to EPINES, configuration EPI41-c. HOTNES internal cavity was lined with borated rubber (red) and the polyethylene shadow-bar was replaced by a multilayer of Teflon (YELLOW) and Aluminium (PURPLE). Blue indicates polyethylene.

The neutron spectra achieved at the reference point of EPINES (centre of the upper cavity, in both EPI22-c or EPI41-c configurations) are reported in Figure 12 (unit spectra, with the purpose of comparing the shape only). The corresponding values of neutron fluence rate are reported in Table 1.

2.2 Assembling EPINES

Below the phases of EPINES assembling:

Figure 7. Aluminium and Teflon disks (2.5 thickness, 20 cm diameter)
Figure 8. Internal cavity lined with borated rubber. Mounting the EPI41-c epithermal filter.
Figure 9. EPI41-c Internal cavity lined with borated rubber and EPI41-c epithermal filter covered with borated rubber.
Fig. 10. Parts of Teflon and Aluminium used to assembly the EPI41-c epithermal cavity.

Fig. 7. Aluminium and Teflon disks (2.5 thickness, 20 cm diameter).

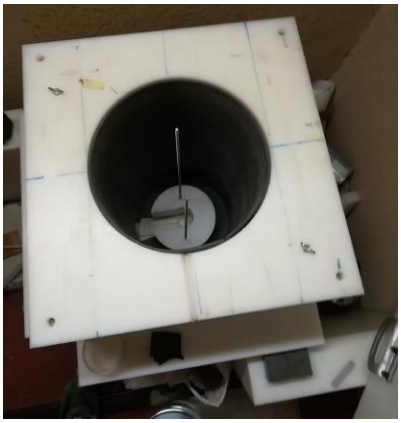

Fig. 8. Internal cavity lined with borated rubber. Mounting the EPI41-c epithermal filter.

Fig. 9. EPI41-c Internal cavity lined with borated rubber and EPI41-c epithermal filter covered with

borated rubber.

Fig. 10. Parts of Teflon and Aluminium used to assembly the EPI41-c epithermal cavity.

2.3 2018 Activity

With the objective of increasing the fraction of epithermal neutrons in the EPINES facility, a further modification scheme was applied to the HOTNES facility, achieving the EPINES – EPILONG configuration. With respect to the EPINES / EPI-41c configuration, the closed irradiation cavity was prolonged (+40 cm) and additional Teflon-aluminium pieces were added to the epithermal column. This is shown in Figure 11. The total length of the irradiation cavity is now 50 cm (from the top of the Teflon/Al column to the facility ceiling). As reference point for the epithermal neutron measurements, that located at height 20 cm from the top of the epithermal column was chosen.

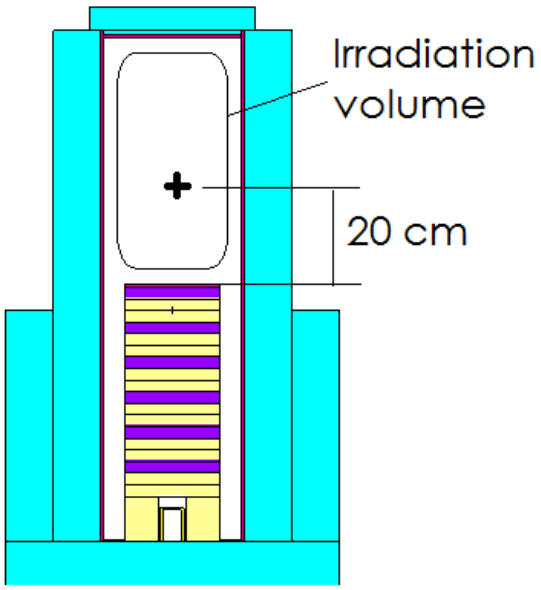

Figure 11. EPINES, configuration EPILONG. The irradiation cavity was prolonged (+ 40 cm) lined with borated rubber (red) and the polyethylene shadow-bar was replaced by a multilayer of Teflon (YELLOW) and Aluminium (PURPLE). Blue indicates polyethylene.

The EPINES / EPILONG spectrum at the ref. point was determined with MCNPX and is reported, compared to the previous EPI22c and EPI41c configurations, in Figure 12. The EPILONG spectrum was also measured experimentally with a set of Bonner spheres recently calibrated with monoenergetic reference fields at NPL (Teddington, UK) [6]. The BSS count rate Vs. Sphere diameter plot, also called "Alevra" plot of the BSS experiment, is shown in Figure 13. The FRUIT code, developed at LNF [7], was used to unfold the experimental data.

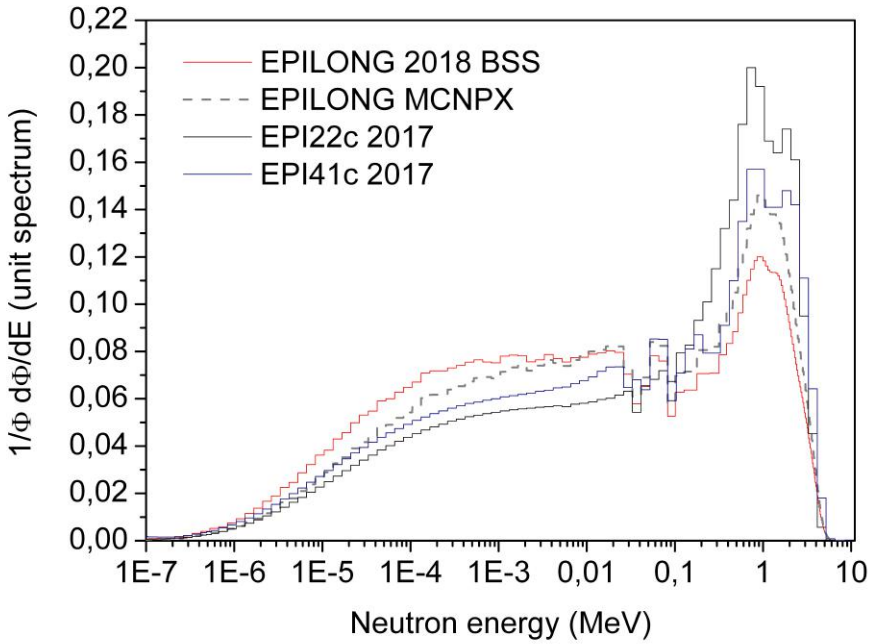

Figure 12. Energy distributions (all in terms of unit spectrum and in lethargy representation) of: EPILONG (ref. point at 20 cm height from the top of the multi-layered column), measured with BSS and MCNPX

simulation; EPI22c (2017) and EPI41c (2017).

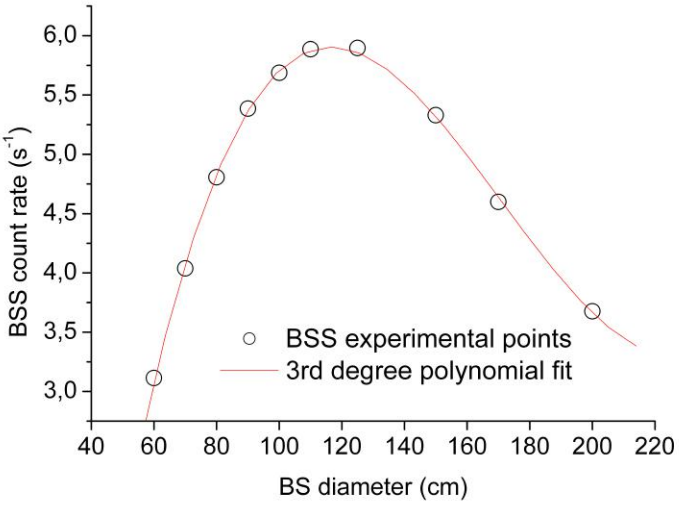

Figure 13. BSS count rate Vs. Sphere diameter plot, also called "Alevra" plot of the BSS experiment to determine the EPILONG neutron spectrum at the reference point (20 cm height from the top of the multi-layered Teflon+Al column). A smooth curve, as demonstrated by the polynomial fit, indicates that measurements are not affected by systematic errors.

With respect to the 2017 EPI22c and EPI41c configurations, the prolonged structure of EPILONG has the effect of improving the spectrum quality, as 70% of the fluence is now in the epithermal domain. As far as the absolute epithermal fluence rate is concerned (Table 1), the EPILONG value (11.3 cm^{-2} s^{-1}) is located in between EPI41-c (7 cm^{-2} s^{-1}) and EPI22c (24.8 m^{-2} s^{-1}).

The reported value of fluence rate and its energy distribution were considered as suited for testing epithermal neutron sensors with unimportant fast neutron response, as those designed for E_LIBANS.

	EPI22-c	EPI41-c	EPILONG
Epithermal fluence rate (cm^{-2} s^{-1})	24.8	7	11.3
Epithermal fraction	51%	58%	70%

Table 1. EPINES spectrum integrated quantities.

The vertical distribution of the epithermal field in EPILONG was also studied, ans resulted to decrease by 2% for every cm of increase in height.

3 Epithermal neutron diagnostics

3.1 Fluence meter with flat-in-energy response

3.1.1 *Design*

The ideal fluence-rate meter for epithermal fields shows a flat response from the eV to 0.1 MeV region, and no response to thermal energies. To design a practical device with similar performance, an extensive MCNPX simulation campaign was undertaken, with starting point the Bonner spheres spectrometer used in the group, and described in Ref. [6]. The central detector is a 11 mm (diameter) x 3 mm (thickness)

^{6}LiI(Eu) scintillator. The sphere with flattest epithermal response is that with diameter 11 cm (BS110 in Fig. 13), but its thermal response is too large, compared with the requirements of monitoring epithermal neutrons only. Thus its response was modified by adding an external one-cm thick layer of borated rubber (^{10}B content is 1.5% in mass), as shown in Fig. 14.

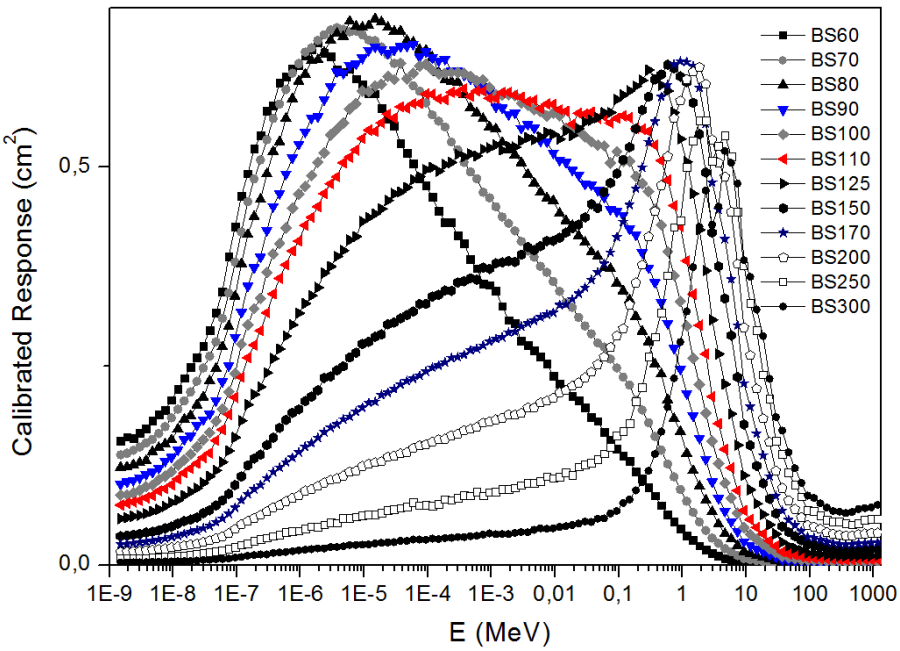

Figure 13. Response matrix of the Bonner sphere spectrometer described in Ref. [6]. The sphere with diameter 11 cm (in red) is that with flattest energy-dependent response in the epithermal domain.

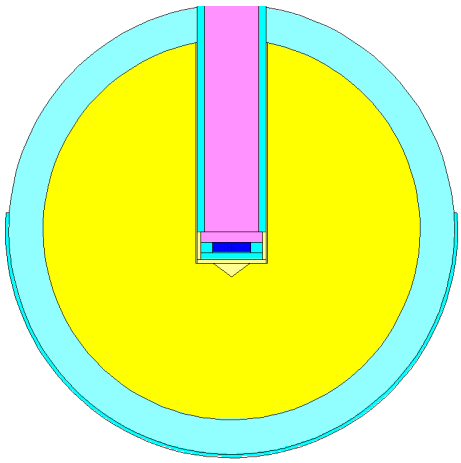

Figure 14. Geometry of the Epi-FM (Epithermal Fluence meter) configuration, achieved by externally covering the 11 cm (in diameter) sphere with a one-cm thick borated rubber layer (^{10}B content is 1.5% in mass).

This new configuration is called Epi-FM (Epithermal Fluence meter) and , compared with the BS110 original response, it shows much lower thermal response and similar degree of constancy in the epithermal domain, see **Fig. 15**.

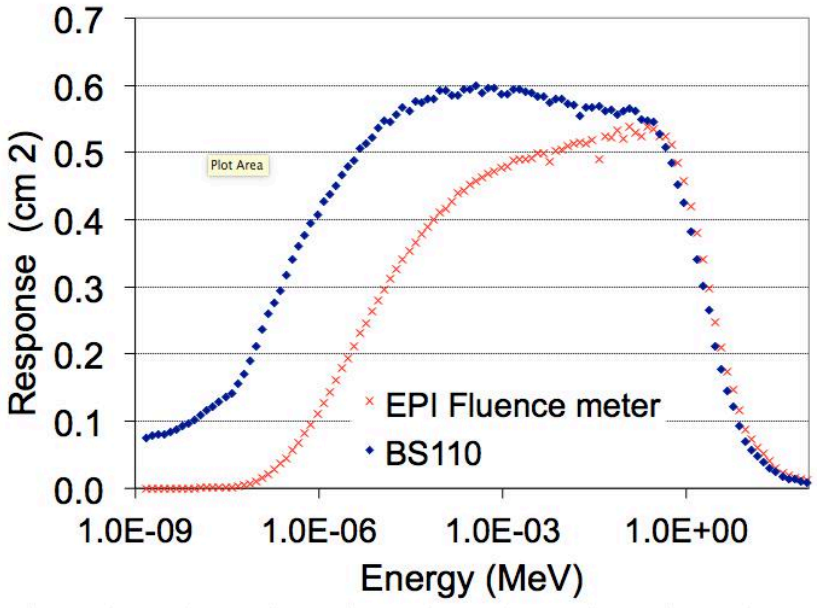

Figure 15. Response matrix of the Epi-FM (Epithermal Fluence meter), compared with that of the BS110 sphere. The central detector is a 11 mm (diameter) x 3 mm (thickness) ^{6}LiI(Eu) scintillator.

3.1.2 *Test in the NPL monoenergetic*

The response function of the Epi-FM (Epithermal Fluence meter) detector, as described in Section **3.1**, was experimentally measured at the NPL Primary metrology Lab (Teddington, UK) with reference monoenergetic neutron fields of energy 144.0 keV, 565.1 keV, and 1.2002 MeV.
The procedure took place with the shadow-cone technique. The delivered fluence was known, via primary standard measurements (long counters), with uncertainty 1.3% at 144 keV, 2.2% at 565 keV, and 2.6% at 1.2 MeV. The EPi-FM device was exposed with and without shadow-cone, to allow correcting for the room-scattered radiation. The experimental response (counts per unit incident fluence) at a given energy E was thus derived as

$$R_{exp}(E) = (C_{tot} / \Phi_{tot} - C_{cone} / \Phi_{cone})$$

Where pedix "cone" and "tot" indicate the exposures with and without shadow cone. The comparison between experimental and simulated (MCNPX) response is given in Table 2.

As shown in the Experiment/simulation column, the Monte Carlo simulation offers a very accurate description of the detector response.

E (keV)	Experimental response (cm^2)	Simulated response (cm^2)	Experiment/simulation
144.0	0.526±0.015	0.530±0.016	0.99±0.04
565.1	0.488±0.013	0.500±0.015	0.98±0.04
1200.2	0.421±0.013	0.415±0.012	1.01±0.04

Table 2. Epi-FM (Epithermal Fluence meter): comparison between experimental and simulated (MCNPX) response at the reference monoenergetic energies 144 keV, 565 keV, and 1.2 MeV available at NPL primary metrology Lab.

3.2 Compact detector for spatial mapping

3.2.1 *Design*

The Epi-FM spherical device is suited for an accurate measurement of the epithermal fluence in a specific point, as the central point of the E_LIBANS epithermal cavity. Nevertheless, due to its size (overall diameter 130 mm), it is unsuited for spatially mapping the epithermal cavity. For this purpose, a point-like detector would be needed. In addition, this point-like detector should not respond to thermal neutrons, possibly contaminating the epithermal field in workplace measurements.
As no point-like epithermal sensors exist on the market, a new configuration (called EPI3) was studied and experimentally tested.
EPI3 is composed by two sandwiched one-cm^2 silicon diodes (*diode 1* and *diode 2*), operating at zero bias voltage. The detectors are separately acquired. D*iode 1* is covered by a 31 μm thick ^{6}LiF neutron radiator and is sensitive to thermal neutrons and, slightly sensitive to photons. By contrast, *diode 2* is covered by a thin Aluminium filter and is in principle sensitive to photons only. By subtracting, channel by channel, the pulse height distribution of Diode 2 from that of Diode 1, only the thermal neutron signal is obtained. To make this sandwiched configuration sensitive to EPITHERMAL neutrons, the following corrections have been implemented:

(1) A one-cubic-cm polyethylene moderator is inserted between diode 1 and diode 2, with the purpose of thermalizing epithermal neutrons and make them visible to diode 1. This is shown in **Fig. 16**.
(2) The diode 1 + diode 2 + one-cubic-cm polyethylene assembly is wrapped with a 5 mm thick borated rubber layer. This filter has an attenuation factor of about 300 for thermal neutrons. The function of this external cover is that of eliminating thermal neutrons originally present in the radiation field. This is shown in **Fig. 17**.

Epithermal neutrons partially penetrate the borated rubber filter and, after thermalization in the one-cubic-cm polyethylene moderator, are detected in diode 1. The gamma rejection is achieved through the differential acquisition of diode 1 and diode 2.
The overall size of the EPI3 sensor is 4.5 cm x 3 cm x 2 cm.
This dimensions are not polit-like but are certainly more suited than Epi-FM to perform spatial mapping of the E_LIBANS epithermal cavity.

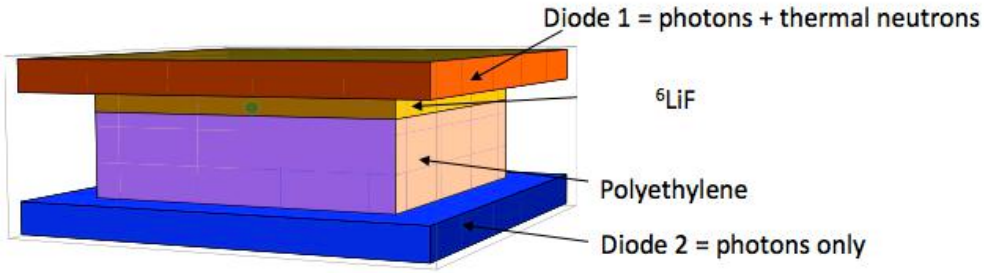

Figure 16. The internal structure of EPI3 detector.

Figure 17. EPI3 detector.

To acquire the signals from diode1 and diode2, a two-channel analogue board (BICE) was designed.
The BICE board includes two separate spectrometry chains, each formed by a CR110 (Cremat) charge preamplifier, followed by a CR200 (Cremat) shaper amplifier with time constant 2 μs. These spectrometry chains share the bias line (not used in this case) and the test signal line. Connectivity is SMA (input signals) and BNC (other).

3.2.2 *Test in the EPILONG facility (INFN-ENEA Frascati)*

The EPI3 detector was calibrated at the reference point (20 cm) of the epithermal field EPILONG (Section 2.3). The acquired spectra of diodes 1 and 2 are reported in **Fig. 18**. As expected, diode 2 spectrum, due to gammas, does not show pulses in the "neutron region", that is above a threshold (0.5 V). By contrast, diode 1 spectrum extends up to about 3 V. The genuine neutron signal is obtained by subtracting diode 2 spectrum from diode 1, and summing all net counts from 0.5 V to 3 V.

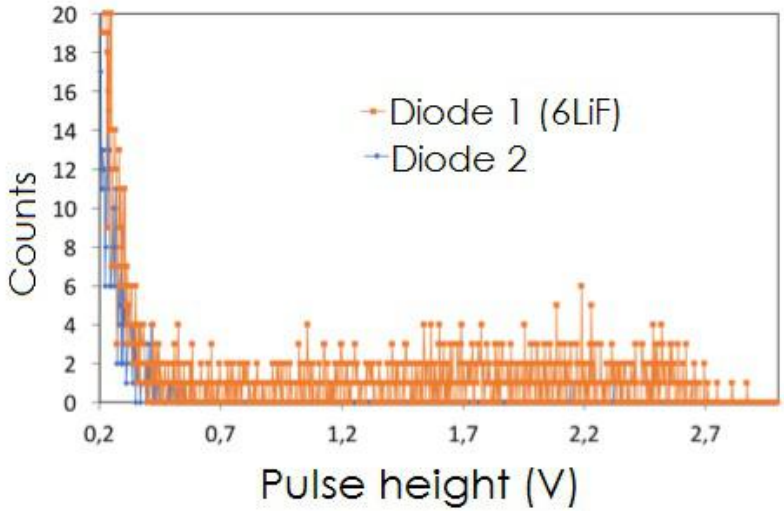

Figure 18. EPI3 spectra acquired at the reference point (20 cm) of the epithermal field EPILONG.

Calibration data are reported in **Table 3**. The epithermal response is obtained by the ratio from epithermal signal and epithermal fluence (10 eV – 100 keV) in EPILONG reference position.

Field	Diode 1 integral > 0.5 V (cps)	Diode 2 integral > 0.5 V (cps)	Epithermal signal (difference) (cps)	Epithermal fluence (cm^{-2} s^{-1})	Experimental epithermal response (cm^2)
EPILONG	(1.08±0.035) E-2	(1.5±0.4) E-2	(1.068±0.039)E-2	11.2±0.3	(9.53±0.45) E-4

Table 3. EPI3 calibration data. The neutron fields used for the calibration were the EPILONG facility (INFN-ENEA Frascati).

In order to check the linearity of EPI3 in terms of the epithermal fluence rate, different acquisitions were performed in EPILONG, by varying the height of the point of test in the irradiation cavity. See **Fig. 19**.

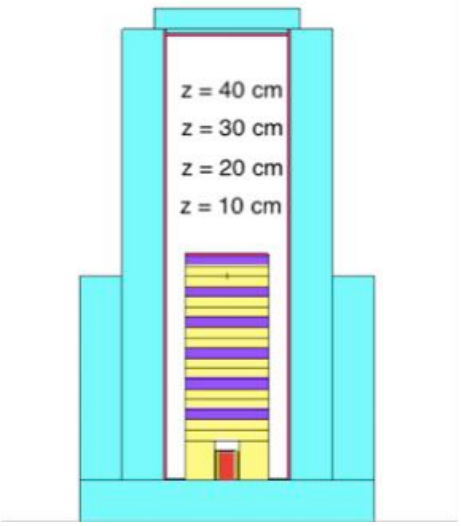

Fig. 19. Measurement points in EPILONG for the EPI3 linearity test.

Reference measurements as function of the height were performed using the fluence meter FM EPi, characterized by flat energy-response. The readings of FM epi and EPi3 as the height varies, normalized to their respective averages, are compared in **Fig. 20**.
As expected, the EPI3 detector shows linear response against the refence detector (FM-Epi).

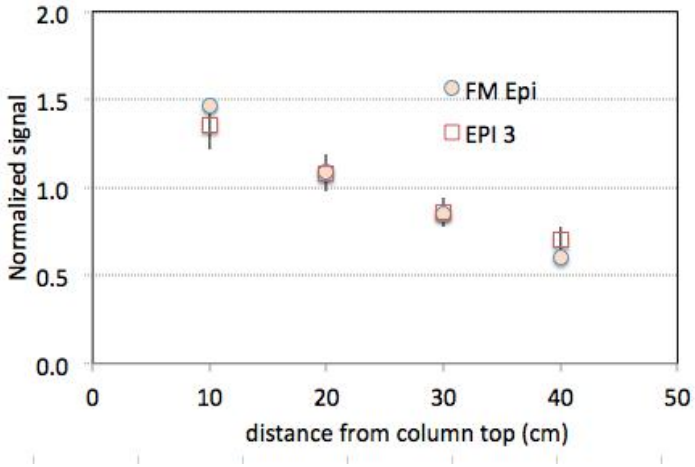

Fig. 20. Readings of FM-epi and EPi3 as the height in EPILONG varies, normalized to their respective averages.

3.2.3 *Test in the NPL monoenergetic fields*

Using the shadow-cone calibration method, as explained in **3.1.2**, the EPI3 sensor was calibrated at the NPL Primary metrology Lab (Teddington, UK) with reference monoenergetic neutron fields of energy 144.0 keV and 565.1 keV. Calibration data are reported in **Table 4**. The EPI3 response is obtained by the ratio from neutron signal and reference monoenergetic fluence. Interestingly, diode 2 shows no response above the 0.5 V threshold, indicating that all genuine "neutron signal" (above 0.5 eV) in diode 1 comes from the LiF radiator.

Field	Diode 1 integral > 0.5 V per unit fluence (cm^2)	Diode 2 integral>0.5V per unit fluence (cm^2)	Experimental response (cm^2)
144 keV	(1.74±0.28) E-4	0	(1.74±0.28) E-4
565 keV	(6.53±0.96) E-5	0	(6.53±0.96) E-5

Table 4. EPi3: calibration data obtained with reference monoenergetic beams 144 keV and 565 keV at NPL primary metrology Lab.

As the moderation efficiency of polyethylene decreases with energy, it is expected that the EPI3 experimental response decreases with energy. The highest response is that measured in EPILONG, having fluence-average energy few keV.

4 4x4 2D array of Silicon Carbide detectors for the spatial mapping of the E_LIBANS thermal field

Figure 21 shows the 3D-printed bi-dimensional array for spatial mapping of the E_LIBANS thermal neutron field with 7 SiC detectors mounted (total 16).

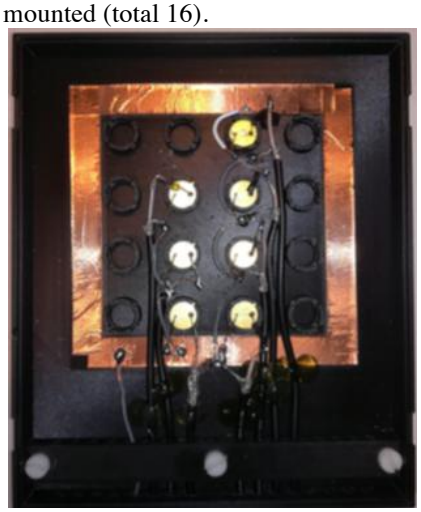

Fig. 21. 3D printed bi-dimensional array for spatial mapping of the E_LIBANS thermal neutron field. Seven SiC detectors are mounted.

Every SiC detector is a 7.6 mm^2 windowless photodiode made sensitive to thermal neutrons through with a 30 micrometre layer of 6LiF. The evaporation-based deposition process is performed at the LNF. Fig. 22 shows the deposited detector.

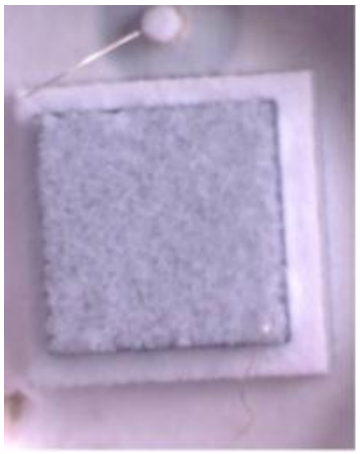

Fig. 22. Sensitive face of the SiC photodiode covered with the neutron radiator (30 micrometre layer of 6LiF).

Every 6LiF-covered SiC detector was individually tested both in pulse mode and in current mode, using well-characterized thermal neutron fields.

Pulse mode: The detector is controlled by a spectrometry chain formed by a CREMAT CR110 charge preamplifier, a CREMAT CR200 shaper amplifier (shaping time 2 μs) and a commercial digitizer (NI USB 6366) operating in streaming mode. Typical pulse height distribution is shown in **Fig. 23**. As the depleted layer at bias level few V is 2-3 micrometre, the neutron-induced charged particles (alpha and Triton) are not stopped in the sensitive layer. With reference to Fig. 23, the main peak at 200 mV refers to charged particles normally impinging the sensitive layer. The tail extending up to 1 V refers to particle with oblique incidence.

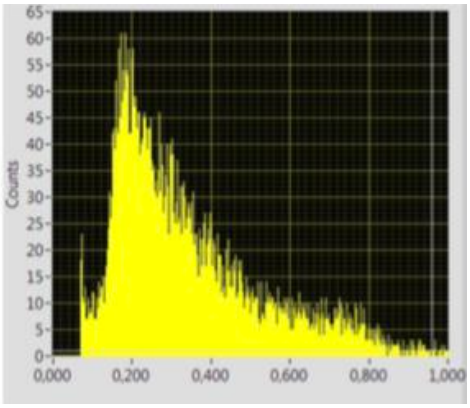

Fig. 23. Typical pulse height distribution of the 6LiF-covered SiC detector exposed to thermal neutrons

Current mode: the unbiased detector is connected to a ultralow-current operational amplifier in trans-resistance configuration. The current generated by the neutron-induced charged particles (alpha and Triton) in the detector is sent to a Gohm feedback resistor, producing a measurable voltage (mV).

The detectors forming the 16-dot 2D array, tested in current and pulse mode, show similar response (standard deviation 10%). An individual response factor was associated to every detector.

5 Publications

[1] M. Costa, E. Durisi, M. Ferrero, V. Monti, L. Visca, S. Anglesio, R. Bedogni, J.M. Gomez-Ros, M. Romano, O. Sans Planell, M. Treccani, D. Bortot, A. Pola, K. Alikaniotis, G. Giannini. Intense thermal neutron fields from a medical-type linac: the e_libans project Radiat. Prot. Dosim, (2018) 180 (1-4) 273-277.

[2] M.Treccani, R. Bedogni, A. Pola, M. Costa, V. Monti, O. Sans Planell, M. Romano, E. Durisi, D. L. Visca, D. Bortot, J.M. Gómez Ros, M. Ferrero, S. Anglesio, G. Giannini, K. Alikaniotis. Developing radiation resistant thermal neutron detectors for the E_Libans project: Preliminary results. Radiat. Prot. Dosim. (2018) 180 (1-4) 304-308.

[3] A. Sperduti, M. Angelone, R. Bedogni, G. Claps, E. Diociaiuti, C. Domingo, R. Donghia, S. Giovannella, J.M. Gomez-Ros, L. Irazola-Rosales, S. Loreti, V. Monti, S. Miscetti, F. Murtas, G. Pagano, M. Pillon, R. Pilotti, A. Pola, M. Romero-Expósito, F. Sánchez-Doblado, O. Sans-Planell, A. Scherillo, E. Soldani, M. Treccani, A. Pietropaolo. Results of the first on the Homogeneous Thermal Neutron Source HOTNES (ENEA/INFN). JINST, 2017 **12** P12029.

[4] R. Bedogni, A. Sperduti, A. Pietropaolo, M. Pillon, A. Pola, J.M. Gómez-Ros. Experimental characterization of HOTNES: A new thermal neutron facility with large homogeneity area. NIM A 843 (2017) 18–21.

[5] R. Bedogni, A. Pietropaolo, J.M. Gomez-Ros. The thermal neutron facility HOTNES: theoretical design. Applied Radiat. Isotopes 127 (2017) 68-72.

[6] R. Bedogni, A. Pola, M. Costa, V. Monti, D.J. Thomas. A Bonner Sphere Spectrometer based on a large ^{6}LiI(Eu) scintillator: Calibration in reference monoenergetic fields. Nuclear Instr. and Methods in Physics Research, A 897 (2018) 18–21.

[7] R. Bedogni, C. Domingo, A. Esposito, F. Fernandez. FRUIT: an operational tool for multisphere neutron spectrometry in workplaces. Nucl. Instr. Meth. A 580, 1301–1309 (2007).